



## Defect states in cubic lutetium oxide caused by oxygen or lutetium inclusions or vacancies

Andrii Shyichuk\*, Eugeniusz Zych

Faculty of Chemistry, University of Wrocław, Joliot-Curie 14, Wrocław, Poland



### ARTICLE INFO

#### Keywords:

Lutetium oxide  
APW + LO  
Defects  
Carrier trapping  
Thermoluminescence

### ABSTRACT

Effects of defect introduction on electronic structure of cubic Ia-3 lutetium oxide ( $\text{Lu}_2\text{O}_3$ ) were characterized by means of density-functional theory calculations using augmented plane wave method with local orbitals (APW + LO) approach. Perdew-Wang 92 local density approximation (LDA) and Räsänen, Pittalis, and Proetto meta-generalized gradient approximation (meta-GGA) density functionals were used. It was found that interstitial oxygen (introduced into the oxygen void available in the structure) and lutetium vacancies result in defect states located about 0.1–0.8 eV above valence band, which can act as hole traps. Oxygen vacancy can act as efficient electron trap, with depth about 1.25 eV. Interstitial lutetium in either  $\text{C}_{3i}$  cation void or in oxygen void results in states located about 0.2–1 eV below conduction band, which can act as electron traps. Both interstitial Lu and Lu vacancies create multiple traps of different depths, which might contribute to experimentally observed trap distributions in  $\text{Lu}_2\text{O}_3$ .

### 1. Introduction

Luminescence phenomena are typically characterized by excited states lifetimes ranging from nano- to milliseconds. In some cases, however, excitation energy can be somehow stored for much longer time within the phosphor material until it is released in form of light. Depending on the lifetime, such phenomena are called afterglow (seconds to minutes), persistent luminescence (hours to days) or permanent energy storage when the excited charge carriers do not dissipate their excessive energy for years or centuries.

Energy storage is typically attributed to trap states in the materials band gap, e.g. between its valence (VB) and conduction (CB) bands. The emission lifetimes in such systems are defined not by the intrinsic lifetime of the emitting level, but by the energy required to detrapp the carriers. The energy is referred as trap depth. Deeper traps correspond to longer lifetimes. If the traps are deep enough, the energy will not be released on its own and can be stored virtually forever; the corresponding materials are called storage phosphors or dosimeters. Increase in temperature of the material, typically up to  $\sim 100$ – $500$  °C, results in energy release and light emission. Such phenomenon is called thermoluminescence (TL).

It was shown [1–5] that materials based on cubic  $\text{Lu}_2\text{O}_3$  can be either afterglow, persistent luminescence or storage phosphors, given that appropriate electron and hole traps are generated via co-doping and/or synthesis conditions. Lutetium oxide materials may also act as

regular scintillator/X-ray phosphors if the traps do not interfere with the luminescence [6–10]. Noteworthy, the two cases are mutually exclusive, as any kinds of delayed emission are deleterious in scintillators. Consequently, accurate design and control of composition and synthesis conditions is required to create a material of desired properties.

Crystal structure of cubic  $\text{Lu}_2\text{O}_3$  [11], space group Ia-3, is characterized by empty sites around  $\text{Lu}^{3+}$  ions suitable for interstitial oxygen incorporation, as well as empty sites (voids) where metal ions can be introduced [8,12]. Per unit cell of 16 formula units of  $\text{Lu}_2\text{O}_3$ , there are the 16 and 32 of such sites, respectively. Consequently, the material is prone to formation of various defects. Hole traps in  $\text{Lu}_2\text{O}_3$  were attributed to interstitial oxygen [3,4], while various sources agree that oxygen vacancies must act as electron traps. High temperature sintering most likely results in oxygen vacancies creation, especially while sintering under vacuum [1]. The two defects may be considered as Frenkel pair [2–4,8]. While defect-free  $\text{Lu}_2\text{O}_3:\text{Eu}^{3+}$  is a potential scintillator, defects in it result in afterglow [3,4], where  $\text{Eu}^{3+}$  dopant ions in the two different Lu sites manifest different activity [13,14]: afterglow radiation is mostly emitted by  $\text{Eu}^{3+}$  in the ( $\text{C}_{3i}$ ) site. Afterglow in  $\text{Lu}_2\text{O}_3:\text{Eu}^{3+}$  can be explained by thermal ionization from multiple hole traps [2].

Doping of  $\text{Lu}_2\text{O}_3$  with  $\text{Tb}^{3+}$  may result in either persistent luminescence or storage phosphor capable of generating thermally- and optically-stimulated emission [1,15,16]. Persistent luminescence of  $\text{Lu}_2\text{O}_3:\text{Tb}^{3+}$  can be improved via sintering under  $\text{N}_2$ - $\text{H}_2$  strongly

\* Corresponding author.

E-mail address: [andrii.shyichuk@chem.uni.wroc.pl](mailto:andrii.shyichuk@chem.uni.wroc.pl) (A. Shyichuk).

reducing atmosphere instead of vacuum [15], and – even more efficiently – via co-dopants, such as Ca, Sr, Ba [15–17]. Similarly, co-doped  $\text{Lu}_2\text{O}_3:\text{Pr},\text{M}$  ( $\text{M} = \text{Ti}, \text{Nb}, \text{Hf}$ ) [17–20] or  $\text{Lu}_2\text{O}_3:\text{Tb},\text{M}$  ( $\text{M} = \text{Ti}, \text{Zr}, \text{Nb}, \text{Hf}, \text{Ta}$ ) [17,20–24] exhibit either storage phosphor properties, or persistent luminescence [25]. The cited papers provide substantial analysis and discussions on storage properties of such materials based on experimental spectroscopic data. Introduction of non-trivalent metals into  $\text{Lu}_2\text{O}_3$  would require a charge compensation. An extended theoretical analysis of defect chemistry in bixbyite oxides was provided [8], indicating, among others, that doping of  $\text{Lu}_2\text{O}_3$  simultaneously with  $\text{Hf}^{4+}$  and  $\text{Tb}^{4+}$  should result in interstitial  $\text{O}^-$  species as charge compensation. On the other hand, experimental results [15] suggest that  $\text{Tb}^{4+}$  formation during synthesis is rather insignificant, while it can be formed via optical excitation [1]. It was argued that the charge compensation occurs via clustering of  $\text{Tb}^{3+}$  ions,  $\text{M}^{2+}$  dopant ions and oxygen vacancies [15].

Summarizing, understanding the nature of the traps and attributing them to particular defects is crucial for clarification of delayed luminescence and energy storage mechanisms in  $\text{Lu}_2\text{O}_3$ -based phosphors [15], as well as improvement and development of new phosphors. In this paper we report results of all-electron DFT calculations of electronic properties of  $\text{Lu}_2\text{O}_3$  with either Lu or O interstitial or vacancy defects. The purpose was to clarify the energies and types of traps that can be created intrinsically in  $\text{Lu}_2\text{O}_3$ , without any extrinsic impurities. Such calculations form a background for further analysis and explanation of properties of doped and co-doped  $\text{Lu}_2\text{O}_3$  materials.

## 2. Computation details

Open source Elk full-potential linearized augmented plane wave (FP-LAPW) code version 4.0.15 was used. The structure of cubic Ia-3  $\text{Lu}_2\text{O}_3$  was obtained from Crystallography Open Database, COD (record number 1537844, original publication: [26]). Augmented plane wave method with additional local orbitals (APW+LO in Wien2k notation) was applied. APW and local orbital settings (defined in species input files for each chemical element, shipped with the code) were Elk defaults. Refer to the Elk reference manual for details. Some of the settings are described below. Lu electron shells from  $1s$  trough  $4d$  were treated as core, while valence shells included  $4f$ ,  $5s$ ,  $5d$  and  $6s$  shells. Oxygen core included only  $1s$  shell, while valence shells were  $2s$  and  $2p$ . Muffin-tin radii for Lu and O were set to 2.05 bohr. Spin-polarized calculations were performed, and a  $2 \times 2 \times 2$  k-point grid was used. This relatively small grid is acceptable as the unit cell of  $\text{Lu}_2\text{O}_3$  is quite large: each of its  $a$ ,  $b$ ,  $c$  dimensions measures as much as 10.396 Å. Radial integration step length (*bradstep* keyword) was 2 instead of default 4, meaning more dense integration grid. Other parameters were Elk defaults, including those defining quality of the calculation: muffin-tin radius (average) times maximum  $|\mathbf{G} + \mathbf{k}|$  (*rgkmax* keyword), which was 7.0 and resulted in maximum  $|\mathbf{G} + \mathbf{k}|$  for APW functions of 3.4146 and maximum  $0.5 \cdot |\mathbf{G} + \mathbf{k}|^2$  of 5.8299. Maximum  $|\mathbf{G}|$  for potential and density (*gmaxvr* keyword) was 12.0 (atomic units). Maximum angular momentum used for APW functions was 8, in the outer part of muffin-tin it was 7 and in the inner part of muffin-tin it was 3. Spin-orbit coupling was added optionally. Perdew-Wang/Cepeley-Alder local density approximation, PW92 [27] and Räsänen, Pittalis, and Proetto meta-generalized gradient approximation, RPP09 [28] functionals were used. With the latter, magnetization axis was fixed in  $z$  direction via setting *cmagz* keyword to *true*. In some cases, in order to induce a high-spin state, external magnetic field of 0.1 at. units along  $z$  axis was applied, using the *bfieldc* keyword.

The calculations completed with no warnings. All linearization energies were found, while core leakages at atoms were about 0.0002 a.u. (O) or  $3 \cdot 10^{-10}$  a.u. (Lu). Total calculated charge error was as large as 0.002 a.u. per total of 2656 electrons in a unit cell of defect-free  $\text{Lu}_2\text{O}_3$ . Consequently, the calculations were considered consistent.

## 3. Results and discussion

### 3.1. Computational methods

In density functional theory (DFT) calculations, energy of the system studied is obtained using functional (a function of a function) of electron density. The density is in turn a function of atomic coordinates and chemical elements at particular positions. Several kinds of approximations apply, which form the corresponding groups of functionals, namely local density approximation, LDA (energy is a function of the density only), generalized gradient approximation, GGA (energy is a function of the density and its gradient) and meta-GGA (energy is a function of the density, its gradient and electron kinetic energy density). Another group is formed by hybrid functionals, in which a portion of exact (Hartree-Fock) exchange is added to the DFT functional.

One of the typical LDA problems is underestimation of material band gaps, especially for insulators. Meta-GGA functionals (in particular RPP09) are said to reproduce band gaps much better, as good as exact exchange or hybrid functionals [28]. On the other hand, meta-GGA is still a pure DFT functional, characterized by much smaller CPU time requirements than the former two. Summarizing, in this study we have used a traditional, well-tested and reliable functional (PW92) and a relatively new and more advanced one (RPP09).

Previous DFT studies of  $\text{Lu}_2\text{O}_3$ -based materials include DFT+U studies (using projector augmented wave pseudopotential method, VASP code and PBE functional) of cell parameters and density of states of defect-free bixbyite (cubic  $\text{Lu}_2\text{O}_3$  [29], structure and electronic properties of  $\text{Lu}_2\text{O}_3$  with interstitial hydrogen [12], dopant-free and Cd-doped cubic  $\text{Lu}_2\text{O}_3$  (with full-potential augmented plane wave plus local orbital, APW+lo and LDA, Wien2k code) [30,31], as well as oxygen vacancies in hexagonal  $\text{Lu}_2\text{O}_3$  (plane wave basis, ultrasoft pseudopotentials, PBE, CASTEP code) [32]. Electronic properties of  $\text{Lu}_2\text{O}_3$  oxides were analyzed using LDA+U and GW approaches, comparing the two (using Wien2k and FHI-gap codes) [33]. No full-scale analysis of defects in  $\text{Lu}_2\text{O}_3$  using APW+LO was provided, despite considerable benefits of the method [33].

Fig. 1 and the other figures below use the same visual style and legend, namely: abscissa axis is energy, while ordinate is density of states; valence band is at lower energy (left), conduction band is at higher energy (right), Fermi level is at zero; dotted and solid lines represent results obtained with or without spin-orbit coupling (SOC), respectively. Positive and negative density corresponds to spin-up and spin-down states, respectively. In contrast to Fig. 1, Figs. 3 and 4 mostly

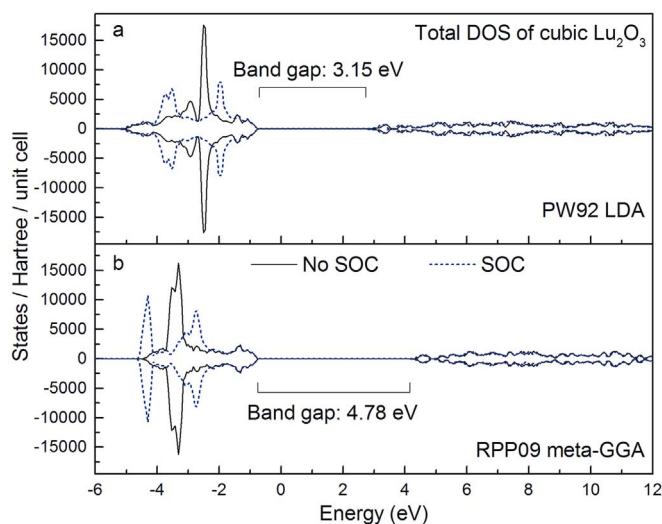


Fig. 1. Total DOS plots of defect-free Ia-3- $\text{Lu}_2\text{O}_3$ , calculated with PW92 (a) and RPP09 (b) functionals.

Download English Version:

<https://daneshyari.com/en/article/7840272>

Download Persian Version:

<https://daneshyari.com/article/7840272>

[Daneshyari.com](https://daneshyari.com)